# Nonequilibrium thermal rectification at the junction of harmonic chains

Sergey V. Dmitriev,[1,2,*] Vitaly A. Kuzkin,[3,4,†] and Anton M. Krivtsov[4,3,‡]
[1]*Institute of Molecule and Crystal Physics, Ufa Federal Research Centre of RAS, Ufa 450054, Russia*
[2]*Ufa State Petroleum Technological University, Ufa 450062, Russia*
[3]*Institute for Problems in Mechanical Engineering RAS, Saint Petersburg 199178, Russia*
[4]*Peter the Great Saint Petersburg Polytechnic University, Saint Petersburg 195251, Russia*

(Received 10 August 2023; accepted 3 November 2023; published 27 November 2023)

A thermal diode or rectifier is a system that transmits heat or energy in one direction better than in the opposite direction. We investigate the influence of the distribution of energy among wave numbers on the diode effect for the junction of two dissimilar harmonic chains. An analytical expression for the diode coefficient, characterizing the difference between heat fluxes through the junction in two directions, is derived. It is shown that the diode coefficient depends on the distribution of energy among wave numbers. For an equilibrium energy distribution, the diode effect is absent, while for non-equilibrium energy distributions the diode effect is observed even though the system is harmonic. We show that the diode effect can be maximized by varying the energy distribution and relative position of spectra of the two harmonic chains. Conditions are formulated under which the system acts as an ideal thermal rectifier, i.e., transmits heat only in one direction. The results obtained are important for understanding the heat transfer in heterogeneous low-dimensional nanomaterials.

DOI: 10.1103/PhysRevE.108.054221

## I. INTRODUCTION

Phonons[1] are the main heat carriers in dielectric solids, and a new field of science and technology referred to as phononics is rapidly developing. The main goal of phononics is to find ways to control the transfer of thermal energy [1–3]. The possibility of creating thermal transistors [4–6], thermal diodes [7–17], and thermal logic devices [18–20] has been demonstrated. Further progress in this area requires better understanding of heat transfer in low-dimensional systems.

The device, called a thermal rectifier (thermal diode), conducts heat differently in opposite directions. It has been shown in a number of works that the thermal diode effect can be achieved in nonlinear systems. The first such idea was to place a nonlinear material with a strong dependence of oscillation frequencies on amplitude between linear materials that do not show such a dependence [21–23]. Another basic idea is to introduce asymmetry into the nonlinear system [9,24–27], which was used, for example, when considering coupled Frenkel-Kontorova chains with different parameters [7]. However, at low temperatures, the effects of nonlinearity are weak and therefore using nonlinearity to achieve the diode effect may be difficult. Then the question arises whether it is even possible to implement a thermal rectifier using linear systems. Answering this question is important, e.g., for the development of efficient methods for the recovery of low-grade thermal energy [28–33].

The presence of the diode effect in linear systems has been debated in the literature. In particular, Kalantar *et al.* argued that harmonic-oscillator chains connecting two harmonic reservoirs at different temperatures cannot exhibit a thermal diode effect, regardless of the structural asymmetry [34]. They referred to the heat flux rectification in harmonic junctions, which they observed during the simulation, as a nonphysical effect [35]. The rectifying effect was not observed in a one-dimensional harmonic chain with a harmonic on-site potential even with a mass gradient, which means that even an asymmetric harmonic system does not guarantee asymmetric heat transfer [36]. Maznev *et al.* argued that the linear structures do not break the reciprocity in reflection and transmission and therefore they cannot show a thermal diode effect [37]. In Ref. [17] it was shown that in an asymmetric nanostructure ballistic phonons do not produce the thermal diode effect under equilibrium conditions, while under nonequilibrium conditions, e.g., described by a displaced Bose-Einstein distribution, a finite diode effect can be achieved. The nonequilibrium heat transfer through a harmonic one-dimensional chain of atoms with a mass impurity in the regime of ballistic phonon transfer was studied, and the possibility of achieving tunable thermal rectification in a completely harmonic system was shown [38]. A thermal rectification mechanism was demonstrated for a harmonic model with a temperature-dependent effective potential [39].

From the works mentioned above, it is clear that in some cases linear systems do not support the thermal diode effect, while in other cases they do. The question arises what the necessary conditions are for the diode effect in harmonic systems. In the present paper, these conditions are derived for a simple one-dimensional model.

Before starting to discuss the diode effect, we briefly mention some relevant facts about heat transport in linear

*dmitriev.sergey.v@gmail.com
†kuzkinva@gmail.com
‡akrivtsov@bk.ru

[1]In the present paper we use the word "phonon" as a synonym for a harmonic wave.

 

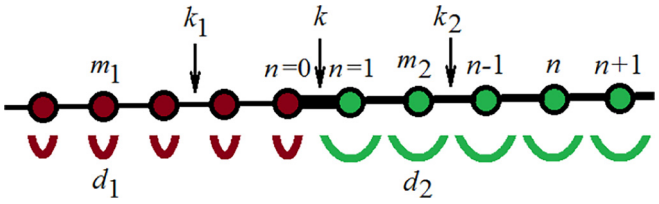


FIG. 1. Junction of semi-infinite harmonic chains of particles with mass $m_i$, connected by bonds of stiffness $k_i$ and interacting with the on-site potential of stiffness $d_i$ ($i = 1, 2$). Particles are numbered by the index $n$. The chains are connected at $n = 0, 1$ by the bond of stiffness $k$. The on-site potential is visualized by brown and green curves showing potential wells.

and nonlinear low-dimensional systems. Many authors have shown that the Fourier thermal conductivity law does not work in defect-free low-dimensional structures. Violation of the Fourier law is manifested, e.g., by the dependence of the effective thermal conductivity coefficient $\kappa$ on the specimen's length $L$ (see, e.g., [40–50]). For linear systems, ballistic heat transport is observed with $\kappa \sim L$ [51–58], while in nonlinear systems there is the so-called anomalous thermal conductivity with $\kappa \sim L^{\alpha}$, where the exponent is in the range $0 < \alpha \leqslant 1$. Thus, since the Fourier law is violated in many low-dimensional systems, the notion of thermal conductivity is defined ambiguously and cannot be used for analysis of the diode effect. Therefore, below we characterize the diode effect in terms of heat (energy) fluxes rather than conductivities.

The main purpose of this study is to investigate the influence of the distribution of energy among phonon modes (wave numbers) on the diode effect in a harmonic asymmetric system and to show how this effect can be maximized. The junction of two harmonic chains with harmonic on-site potentials (elastic foundations) is considered to demonstrate that the thermal diode effect can only be observed if the energy distribution among wave numbers is in nonequilibrium (i.e., nonuniform at high temperatures). The effect is maximal and the system acts as an ideal thermal rectifier when waves with wave numbers in some interval have zero energy and spectra of the chains intersect in a certain way.

## II. MODEL DESCRIPTION

The junction of two semi-infinite harmonic chains with harmonic on-site potentials is described below. Dispersion relations for the chains are derived.

### A. Junction of linear chains

The junction of two semi-infinite harmonic chains with harmonic on-site potential is shown in Fig. 1. The corresponding equations of motion for the chains are

$$m_i\ddot{u}_n = k_i(u_{n-1} - 2u_n + u_{n+1}) - d_i u_n, \quad n \neq 0, 1, \tag{1}$$

where $m_i$, $k_i$, and $d_i$ ($i = 1, 2$) are the mass of particles, the stiffness of the interparticle bonds, and the stiffness of the on-site potential of the $i$th chain, respectively. For chain 1 the equation of motion (1) is valid for $n < 0$ and for chain 2 it is valid for $n > 1$.

For the interfacial particles with $n = 0$ and 1, the equations of motion are

$$m_1\ddot{u}_0 = -k_1(u_0 - u_{-1}) + k(u_1 - u_0) - d_1 u_0, \tag{2}$$

$$m_2\ddot{u}_1 = -k(u_1 - u_0) + k_2(u_2 - u_1) - d_2 u_1. \tag{3}$$

Equations (1)–(3) are considered with initial conditions corresponding to the excitation of waves in one of the chains and zero initial conditions in the other chain. A detailed description of the initial conditions is given in Sec. VI [see Eq. (50)]. Two problems are considered. In the first problem, the vibrations are excited in chain 1 and the energy flux from chain 1 to chain 2 is calculated. In the second problem, the vibrations are excited in chain 2 and the flux from chain 2 to chain 1 is calculated. Using the resulting fluxes from these two problems, we estimate the diode effect (see Sec. IV for details).

We note that since the principle of superposition is fulfilled for the linear system, it is possible to consider the case when both chains are heated. The energy flow from chain 1 to chain 2 will not affect the energy flow in the opposite direction.

As one can see, a very simple harmonic model is analyzed in the present study, while more complicated models have been described in the literature. The interfacial thermal resistance for nanomaterials was discussed in [59]. Advances in the understanding of some phonon phenomena in solid materials are presented in the review in [60]. Heat flow across molecular junctions and the effect of thermal rectification were analyzed for a chain of molecules sandwiched between two solids at different temperatures [61]. The optimal design of the cylindrical thermal rectifier was discussed in [62]. Heat rectification by two qubits [63], strongly interacting spin chains [64], and two interacting classical particles subject to an on-site potential and a Langevin thermal bath [65] was demonstrated. In [66] a method was developed for calculating the thermal conductivity of a classical harmonic lattice with alternating masses and coupling coefficients and interacting with Langevin heat baths. Propagation of phonons, heat transfer, and rectification effect were analyzed for two-dimensional carbon and other materials in [67–74]. Despite the fact that more realistic models for a thermal diode are available in the literature, we decided to limit ourselves to considering a simple toy model in order to demonstrate the effect of energy distribution on the diode effect at a qualitative level.

### B. Dispersion relations for the chains

Looking for the solution to Eq. (1) in the form of a harmonic wave $u_n \sim \exp[\mathrm{i}qn - \mathrm{i}\omega_i(q)t]$ with wave number $q$ and frequency $\omega_i(q)$, we find the dispersion relation for the $i$th chain:

$$\omega_i^2(q) = \frac{d_i}{m_i} + \frac{4k_i}{m_i}\sin^2\frac{q}{2}, \quad i = 1, 2. \tag{4}$$

Here and below only real wave numbers $q$, corresponding to traveling-wave solutions, and positive frequencies are considered. Then according to Eq. (4) the frequencies satisfy

inequalities

$$\omega_i^{\min} \leqslant \omega_i(q) \leqslant \omega_i^{\max},$$
$$\omega_i^{\min} = \sqrt{\frac{d_i}{m_i}}, \quad \omega_i^{\max} = \sqrt{\frac{d_i + 4k_i}{m_i}}. \tag{5}$$

The group velocity, corresponding to Eq. (4), is equal to

$$v_i(q) = a\frac{\mathrm{d}\omega_i}{\mathrm{d}q} = \frac{a}{\sqrt{m_i}}\frac{k_i \sin q}{\sqrt{d_i + 4k_i \sin^2 \frac{q}{2}}}, \quad i = 1, 2, \tag{6}$$

where $a$ is the lattice constant, which is assumed to be the same for both chains. Below we also consider the group velocity as a function of the wave frequency $\Omega$:

$$v_i(\Omega) = \frac{a}{2\Omega}\sqrt{\left(\Omega^2 - \frac{d_i}{m_i}\right)\left(\frac{4k_i + d_i}{m_i} - \Omega^2\right)}. \tag{7}$$

The group velocity vanishes at $\Omega = \omega_i^{\min}$ (for $d_i \neq 0$) and $\Omega = \omega_i^{\max}$. Equations (6) and (7) are further used for calculation of the heat (energy) fluxes and energy transmission coefficient.

## III. PHONON SCATTERING AT THE JUNCTION

Below, the amplitudes of the waves reflected by the junction and transmitted through the junction and the corresponding energy transmission coefficient are calculated.

Referring to Fig. 1, it is assumed that the incident phonon (wave) of amplitude $I$ and wave number $q_1$ travels in chain 1 from the left to the right and hits the junction. This wave is partly reflected and partly transmitted so that the reflected and transmitted waves have the amplitudes $R$ and $T$ and wave numbers $-q_1$ and $q_2$. The frequencies of the incident, reflected, and transmitted waves are equal to each other and are denoted by $\Omega$. Then $q_1$ and $q_2$ are functions of $\Omega$ defined as

$$q_i(\Omega) = 2\arcsin\sqrt{\frac{m_i\Omega^2 - d_i}{4k_i}}, \tag{8}$$

where the principal value of the function $\arcsin(x)$ is taken.

The following ansatz is used to find the amplitudes of the reflected and transmitted waves:

$$u_n = I\sin(q_1 n - \Omega t) - A\sin(q_1 n + \Omega t) + B\cos(q_1 n + \Omega t), \quad n \leqslant 0, \tag{9}$$

$$u_n = C\sin(q_2 n - \Omega t) + D\cos(q_2 n - \Omega t), \quad n \geqslant 1. \tag{10}$$

Equation (9) describes the incident and reflected waves having wave numbers $q_1$ and $-q_1$, respectively, and moving in chain 1. At the same time, Eq. (10) describes the transmitted wave having wave number $q_2$ and moving in chain 2. The parameters $A$, $B$, $C$, and $D$, determining the amplitudes

$$R = \sqrt{A^2 + B^2}, \quad T = \sqrt{C^2 + D^2}, \tag{11}$$

and phases of the reflected and transmitted waves, are to be found. Their derivation is presented in the Appendix and the result is

$$C = \frac{2I\psi k_1 \sin q_1}{\psi^2 + \phi^2}, \quad D = \frac{2I\phi k_1 \sin q_1}{\psi^2 + \phi^2}, \tag{12}$$

where $\phi$ and $\psi$ are determined by the parameters of the chains and frequency $\Omega$ [see Eq. (A7)]. Then the amplitude of the transmitted wave is

$$T = \sqrt{C^2 + D^2} = \frac{2Ik_1 \sin q_1}{\sqrt{\psi^2 + \phi^2}}. \tag{13}$$

Using the formula (13), we calculate the energy transmission coefficient as follows. The average energy fluxes in the incident, transmitted, and reflected waves are equal to

$$j_I = \tfrac{1}{2}m_1 I^2\Omega^2 v_1(\Omega),$$
$$j_T = \tfrac{1}{2}m_2 T^2\Omega^2 v_2(\Omega), \tag{14}$$
$$j_R = -\tfrac{1}{2}m_1 R^2\Omega^2 v_1(\Omega),$$

respectively (these formulas are derived, e.g., in [75]; a discussion of the definition of the flux and group velocity is presented in [76]). The incident wave brings the energy equal to $j_I\Delta t$ to the junction in time $\Delta t$. This energy is divided between the energies of the reflected and transmitted waves, which are equal to $|j_R|\Delta t$ and $j_T\Delta t$, respectively. Then the energy transmission coefficient is defined as [75]

$$\mathcal{T}_e = \frac{j_T}{j_I} = \frac{m_2 v_2(\Omega)T^2}{m_1 v_1(\Omega)I^2}. \tag{15}$$

Here $T/I$ is a function of the wave frequency $\Omega$, given by Eq. (13). Then the transmission coefficient $\mathcal{T}_e$ is a function of $\Omega$. We note that this frequency dependence was also obtained using two different approaches and analyzed in [75]. It was shown in particular that under some conditions the interface is acoustically transparent, i.e., waves with some frequencies pass the junction without reflection.

The formula (15) for the transmission coefficient is valid only if the wave numbers $q_1$ and $q_2$ in the solution given by Eqs. (9) and (10) are real. Then the frequency $\Omega$ should belong to spectra of both chains, i.e., satisfy the inequalities

$$\Omega_{\min} \leqslant \Omega \leqslant \Omega_{\max}, \quad \Omega_{\min} = \max\left(\omega_1^{\min}, \omega_2^{\min}\right), \quad \Omega_{\max} = \min\left(\omega_1^{\max}, \omega_2^{\max}\right), \tag{16}$$

where $\omega_i^{\min}$ and $\omega_i^{\max}$ are defined by Eq. (5). Incident waves with frequencies smaller than $\Omega_{\min}$ or larger than $\Omega_{\max}$ are completely reflected and the corresponding transmission coefficient is equal to zero.

In the following section, we use the expression for the transmission coefficient (15) for estimation of the diode effect.

## IV. THERMAL DIODE EFFECT

Below the diode coefficient is derived for an arbitrary distribution of energy over wave numbers and then some special cases are considered.

### A. Diode coefficient (general formula)

Below we derive the general expression for the diode coefficient, relating fluxes through the junction in two opposite directions. To calculate the diode coefficient two problems are considered.

In the first problem, phonons with some energy distribution among wave numbers are excited only in chain 1, while chain 2 initially has zero energy. Phonons in chain 1 running from

the left to the right are party transmitted through the junction into chain 2 and the energy flux from all such phonons is averaged over a sufficiently long time. This averaged energy flux from chain 1 to chain 2 is designated as $J_{12}$.

In the second problem, phonons are excited only in chain 2, while chain 1 initially has zero energy. The distribution of energy among wave numbers is the same as in the first problem. The flux $J_{21}$ from chain 2 to chain 1 is calculated by switching indices 1 and 2 in the solution of the first problem.

Using solutions of the two problems, we calculate the diode coefficient $\varepsilon$ defined as

$$\varepsilon = \frac{J_{12} - J_{21}}{J_{12} + J_{21}}. \tag{17}$$

If the energy flux is the same in both directions, i.e., $J_{12} = J_{21}$, then $\varepsilon = 0$ and the diode effect is absent. If the fluxes $J_{12}$ and $J_{21}$ are different then the diode effect is present. The system acts as an ideal thermal rectifier ($|\varepsilon| = 1$) if the energy flux in one direction is equal to zero, while the flux in the opposite direction is not.

We calculate the energy flux $J_{12}$ from chain 1, where thermal vibrations are initially excited, to chain 2, which initially has zero energy, as

$$J_{12} = \frac{1}{\pi}\int_0^\pi j_T(q)dq, \tag{18}$$

where $j_T(q)$ is the flux in the transmitted wave, corresponding to the incident wave with wave number $q$, amplitude $I(q)$, and frequency

$$\Omega = \omega_1(q). \tag{19}$$

Then using Eqs. (14) and (15), we obtain

$$j_T(q) = \mathcal{T}_e(\Omega) j_I = \tfrac{1}{2}\mathcal{T}_e(\Omega) m_1 I^2(q)\Omega^2 v_1(\Omega). \tag{20}$$

The amplitude of the incident wave $I(q)$ is related to the average energy per particle $E(q)$ in this wave as

$$I^2(q) = \frac{2E(q)}{m_1\Omega^2}. \tag{21}$$

The function $E(q)$ determines the distribution of energy among wave numbers. This is the key quantity for the present study. The distribution is uniform [$E(q) = \text{const}$] at thermal equilibrium at high temperatures and nonuniform either at low temperatures or far from thermal equilibrium. The case of low temperatures is discussed in Sec. IV E.

Substituting Eqs. (20) and (21) into the expression (18) for the energy flux $J_{12}$, we obtain

$$J_{12} = \frac{1}{\pi}\int_0^\pi \mathcal{T}_e(\Omega)E(q)v_1(\Omega)dq. \tag{22}$$

Then changing the integration variable $q \leftrightarrow \Omega$ in Eq. (22) using Eq. (19) and the definition of the group velocity (6) yields

$$J_{12} = \frac{a}{\pi}\int_{\Omega_{\min}}^{\Omega_{\max}} \mathcal{T}_e(\Omega)E(q_1(\Omega))d\Omega, \tag{23}$$

with the function $q_1(\Omega)$ defined by Eq. (8). Here we use the fact that the transmission coefficient is equal to zero for frequencies outside the interval given by Eq. (16).

The energy flux $J_{21}$ from chain 2 to chain 1 is calculated by switching indices in Eq. (23). Using the fact that the energy transmission coefficient $\mathcal{T}_e(\Omega)$ is invariant with respect to the change of indices $1 \leftrightarrow 2$, we obtain

$$J_{21} = \frac{a}{\pi}\int_{\Omega_{\min}}^{\Omega_{\max}} \mathcal{T}_e(\Omega)E(q_2(\Omega))d\Omega. \tag{24}$$

Then according to (23) and (24), the fluxes $J_{12}$ and $J_{21}$ are generally different, provided the distribution of energy among wave numbers is not uniform, i.e., $E(q)$ is not constant.

Substituting the expressions for $J_{12}$ and $J_{21}$ into the definition (17), we obtain the diode coefficient

$$\varepsilon = \frac{\int_{\Omega_{\min}}^{\Omega_{\max}} \mathcal{T}_e(\Omega)[E(q_1) - E(q_2)]d\Omega}{\int_{\Omega_{\min}}^{\Omega_{\max}} \mathcal{T}_e(\Omega)[E(q_1) + E(q_2)]d\Omega}. \tag{25}$$

Here $q_1$ and $q_2$ are functions of $\Omega$, defined by Eq. (8).

Thus, from Eq. (25) it follows that the diode effect is determined by the transmission coefficient and the distribution of energy among wave numbers. In particular, the diode effect is absent ($\varepsilon = 0$) for a uniform energy distribution, i.e., for $E(q_1(\Omega)) = E(q_2(\Omega)) = \text{const}$. If the energy distribution is nonuniform then the diode coefficient is generally not equal to zero. Further, we use the expression (25) to analyze the diode effect for several particular energy distributions.

### B. Example: Piecewise constant energy distribution

To demonstrate the dependence of the diode coefficient on the energy distribution, we consider the piecewise constant function $E(q)$ such that long and short waves have different energies $E_l$ and $E_s$,

$$E(q) = \begin{cases} E_l, & |q| \leqslant q_* \\ E_s, & q_* < |q| \leqslant \pi, \end{cases} \tag{26}$$

where $q_*$ is the wave number, separating long waves ($|q| \leqslant q_*$) and short waves ($q_* < |q| \leqslant \pi$). To calculate the fluxes through the junction, we substitute the energy distribution (26) into Eq. (22) for $J_{12}$ and into a similar formula for $J_{21}$ and change the integration variable. Then

$$J_{12} \pm J_{21} = \frac{a}{\pi}\left[E_l\left(\int_{\omega_1^{\min}}^{\omega_1^*} \mathcal{T}_e d\Omega \pm \int_{\omega_2^{\min}}^{\omega_2^*} \mathcal{T}_e d\Omega\right) + E_s\left(\int_{\omega_1^*}^{\omega_1^{\max}} \mathcal{T}_e d\Omega \pm \int_{\omega_2^*}^{\omega_2^{\max}} \mathcal{T}_e d\Omega\right)\right],$$
$$\omega_i^* = \omega_i(q_*). \tag{27}$$

From this formula it follows, in particular, that $J_{12} = J_{21}$ for a uniform distribution of energy, i.e., for $E_l = E_s$. For the nonuniform distribution ($E_l \neq E_s$), the diode coefficient depends on the way the spectra of the two chains intersect with each other. For example, we consider the case

$$\omega_1^* \leqslant \omega_2^{\min} < \omega_1^{\max} \leqslant \omega_2^*. \tag{28}$$

The case $\omega_2^* \leqslant \omega_1^{\min} < \omega_2^{\max} \leqslant \omega_1^*$ can be considered similarly by switching indices 1 and 2. Using the formula (27) and the fact that $\mathcal{T}_e \neq 0$ in the interval $(\Omega_{\min}, \Omega_{\max})$ (here $\Omega_{\min} = \omega_2^{\min}$ and $\Omega_{\max} = \omega_1^{\max}$), we show that the diode coefficient is equal to

$$\varepsilon = \frac{E_s - E_l}{E_s + E_l}. \tag{29}$$

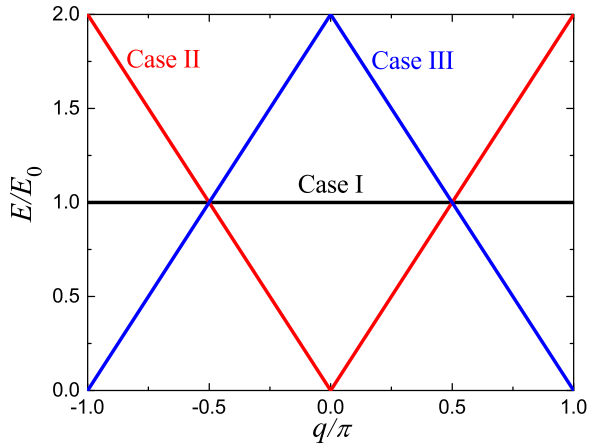


FIG. 2. Three types of energy distribution over phonon modes: case I, all modes have the same energy as in thermal equilibrium at high temperatures; case II, short-wavelength modes have higher energy than long-wavelength ones; case III is opposite to case II. Cases II and III describe nonequilibrium states.

It is seen that in this case the diode coefficient depends only on the distribution of energy and it does not depend on the transmission coefficient. The diode coefficient is also independent of the way the chains are connected with each other (value of stiffness $k$). We note that if either $E_l$ or $E_s$ is equal to zero then the absolute value of the diode coefficient is equal to unity. Therefore, the system acts as an ideal thermal rectifier. More general conditions for ideal thermal rectification are obtained in Sec. V.

### C. Example: Slightly overlapping spectra

We consider the case when the spectra of the two chains overlap slightly, i.e., $\Omega_{\min} \approx \Omega_{\max}$. For example, we restrict ourselves to the case of $\Omega_{\min} = \omega_2^{\min}$ and $\Omega_{\max} = \omega_1^{\max}$. Then $q_1(\Omega) \approx \pi$ in the formula (23) and therefore $E(q_1(\Omega)) \approx E(\pi)$ can be taken out from under the sign of the integral. Using a similar approximation for $J_{21}$, we obtain

$$J_{12} \approx \frac{aE(\pi)}{\pi}\int_{\Omega_{\min}}^{\Omega_{\max}} \mathcal{T}_e d\Omega, \quad J_{21} \approx \frac{aE(0)}{\pi}\int_{\Omega_{\min}}^{\Omega_{\max}} \mathcal{T}_e d\Omega. \tag{30}$$

Then the definition (17) of the diode coefficient $\varepsilon$ yields

$$\varepsilon \approx \frac{E(\pi) - E(0)}{E(\pi) + E(0)}. \tag{31}$$

This formula is valid for an arbitrary distribution of energy among wave numbers. In the case of a piecewise constant distribution of energy it becomes exact and coincides with (29). We note that, as in the previous example, the diode coefficient does not depend on the transmission coefficient.

### D. Example: Linear energy distribution

We analyze the diode effect for three energy distributions over phonon modes shown in Fig. 2. Case I corresponds to high-temperature thermal equilibrium, when the energy of the chain is uniformly distributed among all phonon modes, and cases II and III simulate nonequilibrium states in which it is assumed that the energy of phonon modes varies linearly with the wave number:

$$E(q) = E_0 \quad \text{(case I)}, \tag{32}$$

$$E(q) = 2E_0\frac{|q|}{\pi} \quad \text{(case II)}, \tag{33}$$

$$E(q) = 2E_0\left(1 - \frac{|q|}{\pi}\right) \quad \text{(case III)}. \tag{34}$$

Here $E_0$ is the average energy. In case II the energy of phonons increases with the wave number, while in case III the opposite is true. In other words, in case II (case III), most of the energy of the system belongs to short-wavelength (long-wavelength) phonons.

We set the model parameters

$$\begin{aligned} &m_1 = 1.4, \quad k_1 = 0.7, \quad d_1 = 1.4, \quad m_2 = 1.0, \\ &k_2 = 1.0, \quad d_2 = 0.6, \quad k = 1.3 \end{aligned} \tag{35}$$

and calculate $J_{12}$ and $J_{21}$ using Eqs. (23) and (24) for three cases of energy distribution over phonon modes described by Eqs. (32)–(34) and shown in Fig. 2. Here and below definite integrals are evaluated numerically using Simpson's rule.

TABLE I. Average over all phonon-mode energy fluxes through the junction of two linear chains with the parameters given in Eq. (35), for three cases of energy distribution over the phonon modes shown in Fig. 2. The last column gives the diode coefficient calculated in Eq. (25).

| Case | $J_{12}$ | $J_{21}$ | $\varepsilon$ |
|---|---|---|---|
| I | 0.09707 | 0.09707 | 0.0 |
| II | 0.08688 | 0.07252 | 0.09034 |
| III | 0.1073 | 0.1216 | −0.06270 |

The results are presented in Table I. Notably, the energy flux for case I (uniform distribution) does not depend on the direction of the energy flow and the diode coefficient is equal to zero. For cases II and III the energy flux does depend on the direction of energy flow and the diode effect is observed.

In Fig. 3 the phonon spectra and the energy flux through the junction are analyzed as functions of the wave number $q$. As can be seen in Fig. 3(a), the phonon spectrum of chain 1 is narrower and it is within the spectrum of chain 2. This means that all phonons traveling from chain 1 partly enter chain 2, but the opposite is not true: Only phonons with wave numbers in the range $0.2050 < q/\pi < 0.5634$ are partly transmitted through the junction when they travel from chain 2 to chain 1; otherwise, the conditions (16) are not satisfied. This can be seen in Figs. 3(b)–3(d): The energy flux is nonzero for all phonons traveling from chain 1 to chain 2 and it is nonzero only in the range specified above when traveling from chain 2 to chain 1. However, in case I the areas under the corresponding curves $j_T(q)$ in Fig. 3(b) are exactly the same, meaning that the integrals $J_{12}$ and $J_{21}$ are equal and the diode effect is absent ($\varepsilon = 0$). In nonequilibrium cases II and III [see Figs. 3(c) and 3(d)], the areas under the solid and dashed curves are not equal and the diode effect takes place.

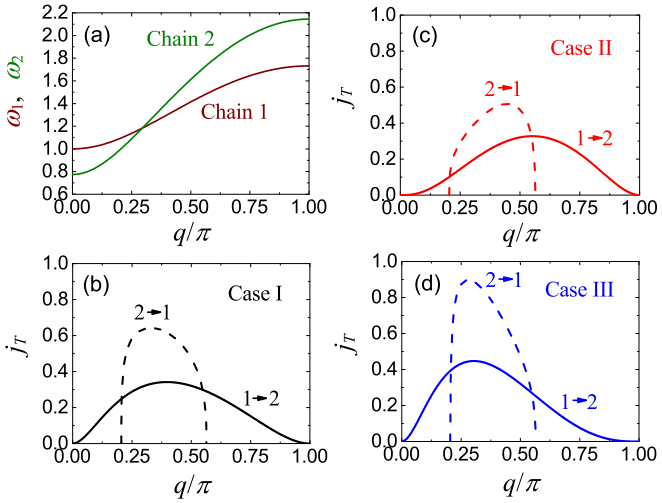


FIG. 3. (a) Phonon dispersion curves for chain 1 and chain 2. The energy flux through the junction [the integrand of Eq. (22)] is plotted as a function of $q$ for (b) case I, (c) case II, and (d) case III. The solid lines correspond to the energy flow from chain 1 to chain 2, while the dashed lines correspond to the energy flow in the opposite direction. The model parameters are given in Eq. (35).

### E. Example: Equilibrium energy distribution corresponding to Bose-Einstein statistics

The nonuniform distribution of energy among wave numbers can be caused, e.g., by quantum effects at low temperatures. In the present section we consider the equilibrium distribution of energy, following from the Bose-Einstein statistics (see, e.g., [77]),

$$E_i(q) = k_B\Theta\varphi\left(\frac{\hbar\omega_i(q)}{k_B\Theta}\right), \quad \varphi(x) = \frac{x}{e^x - 1}, \tag{36}$$

where $k_B$ is the Boltzmann constant, $\Theta$ is temperature, and $\hbar$ is the reduced Planck constant. In the classical limit $\hbar\omega_i/k_B\Theta \ll 1$, the distribution Eq. (36) is uniform, i.e., $E_i \approx k_B\Theta$.

We note that, unlike all previous cases, the energy distribution (36) depends on the dispersion relation of the chain number $i$ and therefore it is generally different for chains 1 and 2. We generalize the derivations, presented in Sec. IV A, to account for this fact. Again, we consider the two problems, described in Sec. IV A, and calculate the fluxes $J_{12}$ and $J_{21}$. However, in this section we assume that in the two problems the initial vibrations are excited with the same $\Theta$ rather than the same total energy. Then, using the same reasoning as in Sec. IV A, we obtain the expression for the flux

$$\begin{aligned} J_{12} &= \frac{1}{\pi}\int_0^\pi \mathcal{T}_e E_1(q)v_1(q)dq \\ &= \frac{k_B\Theta}{\pi}\int_0^\pi \mathcal{T}_e\varphi\left(\frac{\hbar\omega_1(q)}{k_B\Theta}\right)v_1(q)dq. \end{aligned} \tag{37}$$

Then change of the integration variable in Eq. (37) yields

$$J_{12} = \frac{ak_B\Theta}{\pi}\int_{\Omega_{\min}}^{\Omega_{\max}} \mathcal{T}_e(\Omega)\varphi\left(\frac{\hbar\Omega}{k_B\Theta}\right)d\Omega. \tag{38}$$

The right-hand side of this expression is invariant to the switching of the indices 1 and 2 and therefore the fluxes in both directions are equal, i.e., $J_{12} = J_{21}$ and $\varepsilon = 0$.

Thus, under the equilibrium energy distribution (36), the diode effect is absent at all temperatures. A similar result was obtained in [17] for a more complicated system using a kinetic model of heat transfer and the Landauer-Büttiker formalism. We also note that the diode effect is absent for a large class of energy distributions that can be obtained by changing $\varphi(x)$ in Eq. (36) by an almost arbitrary function.[2]

## V. MAXIMAL THERMAL DIODE EFFECT

The conditions for the maximum thermal diode effect are derived and discussed below.

### A. Conditions for an ideal thermal rectifier

We obtain conditions corresponding to the maximum possible thermal diode effect ($|\varepsilon| = 1$). From the definition (17) it follows that the diode coefficient $\varepsilon$ is equal to 1 if $J_{21} = 0$ and $J_{12} \neq 0$. In other words, the energy transport is possible only from chain 1 to chain 2. Consider the formula (24) for the flux $J_{21}$. The formula contains an integral of the product of non-negative functions $\mathcal{T}_e(\Omega)$ and $E(q_2(\Omega))$. Since $\mathcal{T}_e$ is generally not equal to zero in the interval $(\Omega_{\min}, \Omega_{\max})$ then the flux $J_{21}$ vanishes only if $E(q_2(\Omega))$ is equal to zero for all frequencies in this interval. Combining this with the condition $J_{12} \neq 0$, we obtain

$$\varepsilon = 1 \Leftrightarrow \begin{cases} E(q) = 0 \,\forall\, q \in (q_2(\Omega_{\min}), q_2(\Omega_{\max})) \\ \int_{\Omega_{\min}}^{\Omega_{\max}} \mathcal{T}_e(\Omega)E(q_1(\Omega))d\Omega \neq 0, \end{cases} \tag{39}$$

with the functions $q_i(\Omega)$ defined in Eq. (8). Similar conditions for $\varepsilon = -1$ are obtained by switching indices 1 and 2 in the formula (39).

Thus the system acts as an ideal thermal rectifier if waves with wave numbers corresponding to the passband [i.e., interval $(\Omega_{\min}, \Omega_{\max})$] have zero energy for one chain and nonzero energy for another chain. This condition is satisfied, e.g., in the case when energies of either short or long waves are equal to zero. These two particular cases are considered below.

### B. Example: Short or long waves having zero energy

We begin with the case when short waves are absent, i.e.,

$$E(q) = \begin{cases} f_l(|q|), & |q| \leqslant q_* \\ 0, & q_* < |q| \leqslant \pi, \end{cases} \tag{40}$$

where $f_l(|q|)$ is a non-negative function, describing the distribution of energies of long waves. In this case, the general conditions for ideal thermal rectification (39) are simplified as follows. Since the function $q_2(\Omega)$ is monotonically increasing in the interval $[0, \pi]$, then the first condition from (39) is satisfied if $q_2(\Omega_{\min}) > q_*$ and hence $\Omega_{\min} > \omega_2(q_*)$. The

[2]The only formal restriction on the function $\varphi$ in Eq. (36) is that it should be non-negative with a finite integral with respect to the wave number in order to guarantee that the total energy per particle is also finite.

second condition from (39) yields $\Omega_{\min} < \omega_1(q_*)$. Then the conditions (39) can be replaced by $\omega_2(q_*) < \Omega_{\min} < \omega_1(q_*)$. These inequalities are satisfied only for $\Omega_{\min} = \omega_1^{\min}$. Therefore, Eq. (39) reduces to

$$\varepsilon = 1 \Leftrightarrow \omega_1^{\min} > \omega_2(q_*). \tag{41}$$

This condition can also be rewritten in terms of wave numbers as

$$\varepsilon = 1 \Leftrightarrow q_2\left(\omega_1^{\min}\right) > q_*. \tag{42}$$

A similar condition for $\varepsilon = -1$ is obtained from Eq. (41) by switching indices 1 and 2.

Similarly, we consider the case when long waves have zero energy, i.e.,

$$E(q) = \begin{cases} 0, & |q| \leqslant q_* \\ f_s(|q|), & q_* < |q| \leqslant \pi, \end{cases} \tag{43}$$

where $f_s(|q|)$ is a non-negative function, describing the distribution of energy of short waves. Using the same reasoning as in the previous case, we obtain

$$\varepsilon = 1 \Leftrightarrow \omega_1^{\max} < \omega_2(q_*) \tag{44}$$

and

$$\varepsilon = 1 \Leftrightarrow q_2\left(\omega_1^{\max}\right) < q_*. \tag{45}$$

Thus the system acts as an ideal thermal rectifier if no energy is stored in short or long waves and the spectra of the chains intersect in such a way that Eq. (41) or (44), respectively, is satisfied, while the functions $f_l$ and $f_s$ can be chosen arbitrary. We note that the conditions (41) can only be satisfied if chain 1 has the on-site potential.

### C. Example: Linear energy distribution

Below we show that the absolute value of the diode coefficient can be large even if the energy distribution $E(q)$ is equal to zero only at one point. For this purpose, linear distributions (33) and (34) are considered.

We vary the relative positions of the spectra of the two chains and calculate the diode coefficient $\varepsilon$ using Eq. (25). The parameters of chain 2 (and therefore its spectrum) are fixed:

$$m_2 = 1.0, \quad k_2 = 1.0, \quad d_2 = 0.6. \tag{46}$$

From Eq. (5) we find the minimum and maximum phonon frequencies as well as the width of the phonon spectrum of chain 2,

$$\omega_2^{\min} = \sqrt{0.6} \approx 0.775, \quad \omega_2^{\max} = \sqrt{4.6} \approx 2.145,$$
$$\Delta\omega_2 = \omega_2^{\max} - \omega_2^{\min} \approx 1.370. \tag{47}$$

For chain 1 we set $m_1 = 1$ and change the stiffness of the on-site potential $d_1$ (and therefore $\omega_1^{\min}$), keeping the width of the phonon spectrum unchanged:

$$\Delta\omega_1 = \omega_1^{\max} - \omega_1^{\min} = \sqrt{3} - 1 \approx 0.732. \tag{48}$$

Then the stiffness $k_1$ is calculated as

$$k_1 = \frac{m_1}{4}\Delta\omega_1\left(\Delta\omega_1 + 2\omega_1^{\min}\right) \approx 0.1876 + 0.4331\sqrt{d_1}. \tag{49}$$

The stiffness of the spring connecting the chains is, as always, $k = 1.3$.

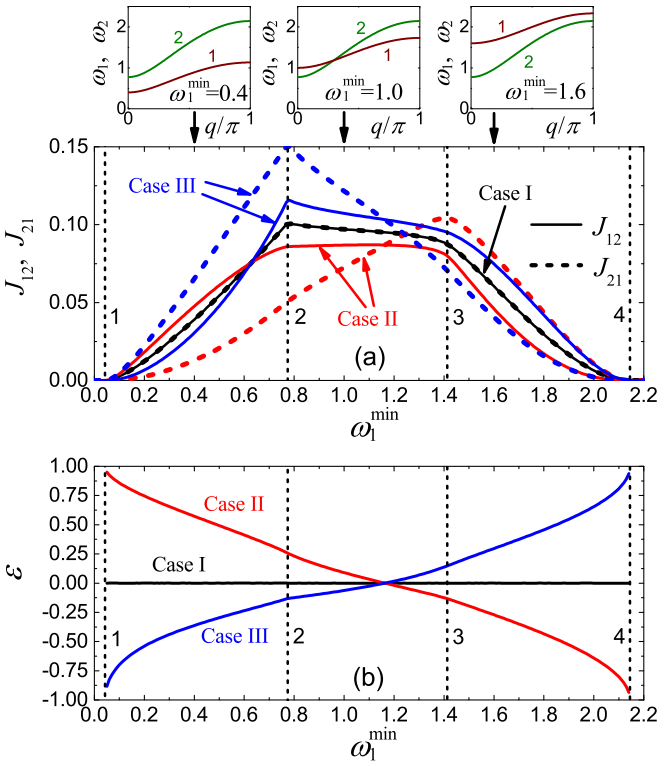


FIG. 4. Dependence of (a) the energy flux through the junction and (b) the diode coefficient on the relative position of the phonon spectra of two harmonic chains. The spectrum of chain 2 is fixed and the position of the spectrum of chain 1 is determined by the minimum frequency $\omega_1^{\min}$, while the width of the spectrum remains constant [see Eq. (48)]. Three top panels in (a) show phonon spectra for particular values of $\omega_1^{\min}$. Solid and dashed curves in (a) show $J_{12}$ and $J_{21}$, respectively. Black, red, and blue lines in (a) and (b) show the results for the three cases of energy distribution over phonon modes (see Fig. 2). The meaning of the vertical dashed lines numbered 1–4 is explained in the text.

In Fig. 4(a), depending on $\omega_1^{\min}$, the energy fluxes through the junction are shown by the solid ($J_{12}$) and dashed ($J_{21}$) lines. The black, red, and blue curves correspond to three different energy distributions over phonon modes given by Eqs. (32), (33), and (34), respectively (see Fig. 2). The top three panels show the phonon spectra of chains 1 and 2 for specific values of $\omega_1^{\min} = 0.4$, 1.0, and 1.6, when the spectrum of chain 1 overlaps with the lower part of the spectrum of chain 2, is within the spectrum of chain 2, and overlaps with the upper part of the spectrum of chain 2, respectively. The four vertical dashed lines numbered 1, 2, 3, and 4 in Figs. 4(a) and 4(b) correspond to the cases $\omega_1^{\max} = \omega_2^{\min}$, $\omega_1^{\min} = \omega_2^{\min}$, $\omega_1^{\max} = \omega_2^{\max}$, and $\omega_1^{\min} = \omega_2^{\max}$, respectively.

The results shown in Fig. 4(a) confirm that in case I with a uniform energy distribution over phonon modes $J_{12} = J_{21}$, but for nonequilibrium cases II and III, i.e., for nonuniform distributions of energy over phonon modes, the energy flux depends on the direction. In Fig. 4(b) the diode coefficient is shown as a function of $\omega_1^{\min}$ with black, red, and blue curves for cases I, II, and III, respectively. In case I $\varepsilon = 0$, which means that in thermal equilibrium the diode effect is absent for any mutual arrangement of the phonon spectra of the chains.

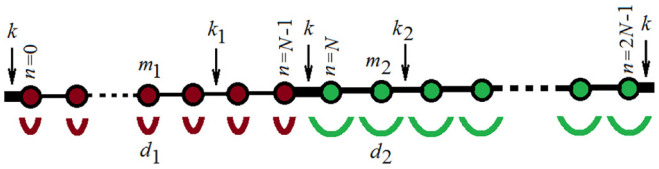


FIG. 5. Numerical simulation model: two harmonic chains of $N$ particles under periodic boundary conditions $u_n = u_{n+2N}$. The chains are connected by bonds of stiffness $k$. The chain parameters are particle mass $m_i$, bond stiffness $k_i$, and on-site potential stiffness $d_i$ $(i = 1, 2)$.

In nonequilibrium cases II and III, the diode effect is observed, i.e., $\varepsilon \neq 0$.

Note the diode coefficient $\varepsilon$ vanishes for some value of $\omega_1^{\min}$, which is the same for cases II and III. This fact is explained as follows. For energy distributions (33) and (34), corresponding to cases II and III, numerators in the expression for the diode coefficient (25) differ only by a sign and therefore they vanish simultaneously.

We also note that the phonons with wave vectors approaching the boundary of the first Brillouin zone have a group velocity approaching zero [see Eq. (6)]. Therefore, ideal thermal rectification is achieved in the limit of vanishing overlap of the phonon spectra of two chains, when the energy flux through the junction also vanishes. This means that for practical applications, a trade-off must be considered when the two spectra overlap enough to have a noticeable heat flux but not too much to have a large diode coefficient.

Summing up, for any mutual arrangement of the phonon spectra of two chains, the diode effect is present only for nonequilibrium energy distributions (cases II and III). As follows from Fig. 4(b), the diode effect is small when one of the spectra is inside the other. On the other hand, the diode effect is maximal and $\varepsilon$ approaches the maximum values $\pm 1$, predicted by the approximate formula (31), when the phonon spectra of two chains overlap only near their edges.

## VI. NUMERICAL RESULTS

In this section we confirm the analytical results obtained above by numerical simulations. In simulations, chains 1 and 2 are finite and form a periodic cell of $2N$ particles, i.e., the conditions $u_n = u_{n+2N}$ are satisfied. Particles $n = 0, \ldots, N-1$ belong to chain 1, while particles $n = N, \ldots, 2N-1$ belong to chain 2. Under periodic boundary conditions, there are two junctions between the chains (springs between particles $N-1$ and $N$ and between particles 0 and $2N-1$) (see Fig. 5).

It is assumed that at $t = 0$ chain 1 is heated and chain 2 has zero energy. For $t > 0$ energy starts to flow from chain 1 to chain 2. Initial conditions for chain 1 are formulated as the sum of $N/4$ phonon modes numbered by the index $i = 1, \ldots, N/4$ [78],

$$u_n = I_{N/4}\cos(\pi n) + \sum_{i=1}^{N/4-1} I_i \cos[p_i n \pm \omega_1(p_i)t + \Delta_i], \quad (50)$$

where $n = 0, \ldots, N-1$. The $i$th harmonic has wave number $p_i = 4\pi i/N$, frequency $\omega_1(p_i)$, random phase shift $\Delta_i$ uniformly distributed in the interval $(0, 2\pi)$, and amplitude $I_i^2 = 2E(p_i)/Nm_1\omega_1(p_i)^2$. The amplitude is chosen such that the harmonic has energy $E(p_i)$. Phase shifts of different harmonics are uncorrelated, i.e., $\langle \Delta_i \Delta_i \rangle = 0$ for $i \neq j$, where $\langle \cdots \rangle$ stands for mathematical expectation. The plus or minus sign in front of the $\omega_1(p_i)t$ term is taken with equal probability in order to have an equal contribution to the energy from the waves running to the right and to the left. Initial displacements of the particles are calculated using Eq. (50) at $t = 0$, while initial velocities are calculated as time derivative of Eq. (50) at $t = 0$. The considered distributions of energy over phonon modes are given by Eqs. (32)–(34) and are shown in Fig. 2.

TABLE II. Numerically found energy fluxes through the junction of two linear chains with the parameters given in Eq. (35) for three cases of energy distribution over the phonon modes shown in Fig. 2. The last column gives the diode coefficient defined in Eq. (17).

| Case | $J_{12}$ | $J_{21}$ | $\varepsilon$ |
|---|---|---|---|
| I | 0.09762 | 0.09732 | 0.00154 |
| II | 0.08697 | 0.07299 | 0.08740 |
| III | 0.1076 | 0.1217 | −0.06149 |

Simulations are carried out for $2N = 4096$ and model parameters given by Eq. (35). The equations of motion (1)–(3) are integrated numerically with the use of the symplectic sixth-order Störmer method [79] with time step equal to $10^{-2}$.

In simulations, the total energy of the chain 2 is calculated as

$$E_2 = \sum_{n=N}^{2N-1} \epsilon_n, \quad (51)$$

where the energy per $n$th particle is defined as

$$\epsilon_n = \frac{m_2}{2}\dot{u}_n^2 + \frac{k_l}{4}(u_n - u_{n-1})^2 + \frac{k_r}{4}(u_{n+1} - u_n)^2 + \frac{d_2}{2}u_n^2. \quad (52)$$

Here $k_l$ and $k_r$ are the stiffnesses of the bonds connecting the $n$th particle with the left and right neighbors, respectively. The first term on the right-hand side of this expression gives the kinetic energy of the $n$th particle, the second and the third terms describe the halves of the potential energies of the left and right bonds of the $n$th particle, and the fourth term is the energy of interaction of the $n$th particle with the on-site potential.

In Fig. 6 the curves $E_2(t)$ averaged over 500 realizations are shown by the thick solid lines. It can be seen that $E_2$ increases almost linearly with time. The slopes of the solid lines give $2J_{12} = \mathrm{d}E_2/\mathrm{d}t$ [the factor 2 is introduced to account for the presence of two junctions in the finite-size chain with the periodic boundary conditions (see Fig. 5)]. The calculated values of $J_{12}$ are presented in Table II. Then the model parameters are switched, i.e., $m_1 \leftrightarrow m_2$, $k_1 \leftrightarrow k_2$, and $d_1 \leftrightarrow d_2$, and the dashed lines presented in Fig. 6 are obtained by averaging over 500 realizations. From these lines the fluxes are found as $2J_{21} = \mathrm{d}E_2/\mathrm{d}t$ and are also presented in Table II. The diode coefficient $\varepsilon$ is calculated using Eq. (17). The thin lines in Fig. 6(b) show the time evolution of $E_2$ for the energy flow

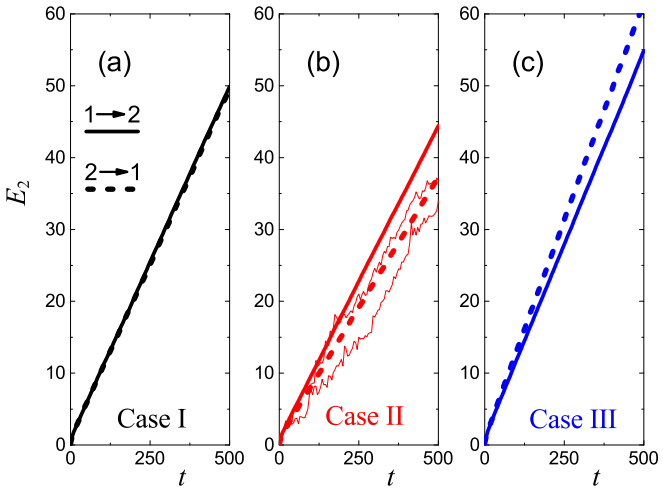


FIG. 6. Energy of chain 2 as a function of time averaged over 500 realizations. The results for the three different energy distributions over the phonon modes shown in Fig. 2 are presented for (a) case I, (b) case II, and (c) case III. The slopes of the thick solid lines correspond to the energy fluxes $J_{12}$ and the dashed lines to the fluxes $J_{21}$. Thin lines in (b) show two particular realizations to give an idea of the dispersion of simulation results.

$2 \to 1$ for two particular realizations to give an idea of the dispersion of simulation results.

A comparison of the numerical results presented in Table II with the analytical results presented in Table I shows fairly good agreement. In case I, $J_{12}$ is equal to $J_{21}$ within the simulation accuracy, and in nonequilibrium cases II and III, the energy flux depends on the direction, i.e., the diode effect is realized.

## VII. CONCLUSION

The thermal diode effect has been analyzed for the junction of two harmonic chains. The expression for the diode coefficient, which relates the heat (energy) fluxes through the junction in the two opposite directions, was derived analytically. It was shown that the diode effect is determined by the transmission coefficient and the distribution of the transmitted energy among the wave numbers (phonon modes). In particular, for any mutual arrangement of the phonon spectra of the chains, the diode effect is absent if the energy distribution among the phonon modes is in equilibrium (uniform or according to Bose-Einstein statistics). For nonequilibrium energy distributions, the thermal diode effect can be observed in the harmonic system. Several examples of such distributions were given and the corresponding diode coefficients were calculated.

The physical explanation for the diode effect in the harmonic system is as follows. The energy is transmitted through the junction by harmonic waves with frequencies in the passband (intersection of the spectra of the chains). For each chain, the passband determines the interval of wave numbers that contribute to the flux through the junction. Since the dispersion relations of the chains are different, these intervals are also different for chains 1 and 2. Therefore, for nonuniform energy distribution, the amount of energy in the waves that can pass through the junction is generally different for chains 1 and 2. This difference causes the diode effect in the harmonic system.

It should be noted that perfect thermal rectification is achieved in the limit of vanishing overlap of the phonon spectra of two chains, when the energy flux through the junction also tends to zero. This means that in practice a trade-off is unavoidable: The two spectra must overlap enough to have a noticeable heat flux but not too much to have a large diode coefficient.

It has been shown that the system acts as an ideal thermal rectifier (the energy is transferred through the junction in only one direction) if the energy distribution satisfies the conditions given by Eq. (39). The conditions are such that waves with wave numbers corresponding to the passband have zero energy for one chain and nonzero energy for another chain. In particular, the conditions are satisfied if the energies of either short or long waves are zero and the spectra of the chains satisfy Eq. (41) or (44). Note that the conditions (41), corresponding to the case of no short waves, can only be satisfied if one chain has an on-site potential.

Our results reveal the possible reason why some harmonic systems exhibit a thermal diode effect [38,39,80] and others do not [17,34–37]; the difference in the results can be related to the proximity of the considered system to thermal equilibrium. The results also suggest that the distribution of energy among normal modes can be used to maximize the thermal diode effect.

A possible practical realization of a thermal rectifier based on the results obtained could be the use of low-pass and high-pass filters for the heat coming from the left and right sides at the junction of the two chains.

The results presented have been obtained for a purely harmonic model. The nonlinearity, which may be weak but is always present in real crystals, leads to at least two physical processes that are absent in the harmonic model, namely, redistribution of energy among wave numbers and transition from ballistic to anomalous or diffusive heat transfer. However, both of these processes require some time to manifest, depending on the nonlinearity [81–84]. During this time the behavior of the weakly nonlinear system is approximately described by the harmonic theory, developed, e.g., in the works in [85–88]. Therefore, we believe that the results presented are applicable to weakly nonlinear systems on a certain timescale. However, these qualitative considerations should be confirmed by a detailed analysis, which is beyond the scope of the present paper.

In this work, a model with deterministic energy distributions $E(q)$ was considered. We believe that uncorrelated, normally distributed fluctuations of phonon energies would lead to the same physical picture and that only a colored noise might give a qualitatively new behavior of the system [89]. We would like to leave this interesting and nontrivial question to future studies.

## ACKNOWLEDGMENTS

The authors are grateful to S. N. Gavrilov, S. D. Lyazhkov, and A. A. Sokolov for useful discussions. This work was

supported by the Russian Science Foundation, Grant No. 23-11-00364.

## APPENDIX

The reflection and transmission of a phonon wave incident on the junction of harmonic chains is described by the ansatz (9) and (10). To find the relation between $A, B, C, D$ and the amplitude of the incident wave $I$, we substitute Eqs. (9) and (10) into Eqs. (2) and (3), use the identities $\sin(x+y) = \sin x \cos y + \cos x \sin y$ and $\cos(x+y) = \cos x \cos y - \sin x \sin y$, and demand that the terms with $\sin(\Omega t)$ and $\cos(\Omega t)$ cancel separately. Then the following four equations for $A$, $B$, $C$, and $D$ are obtained:

$$\gamma A + k_1 B \sin q_1 - k(C \cos q_2 - D \sin q_2) = -\gamma I, \quad \text{(A1)}$$

$$k_1 A \sin q_1 - \gamma B + k(C \sin q_2 + D \cos q_2) = k_1 I \sin q_1, \quad \text{(A2)}$$

$$kA - \delta C + \theta D = -kI, \quad \text{(A3)}$$

$$kB - \theta C - \delta D = 0. \quad \text{(A4)}$$

Here

$$\begin{aligned} \beta &= k + k_2 + d_2, \\ \gamma &= k + k_1(1 - \cos q_1) + d_1 - m_1\Omega^2, \\ \delta &= (\beta - m_2\Omega^2)\cos q_2 - k_2 \cos(2q_2), \\ \theta &= (\beta - m_2\Omega^2)\sin q_2 - k_2 \sin(2q_2). \end{aligned} \quad \text{(A5)}$$

Excluding $A$ and $B$ from Eqs. (A1) and (A2) with the help of Eqs. (A3) and (A4), we obtain

$$\begin{aligned} -\phi C + \psi D &= 0, \\ \psi C + \phi D &= 2k_1 I \sin q_1, \end{aligned} \quad \text{(A6)}$$

where

$$\begin{aligned} \phi &= -\delta\frac{\gamma}{k} - \theta\frac{k_1}{k}\sin q_1 + k\cos q_2, \\ \psi &= -\theta\frac{\gamma}{k} + \delta\frac{k_1}{k}\sin q_1 + k\sin q_2. \end{aligned} \quad \text{(A7)}$$

Solving Eq. (A6), we obtain the expressions (12) for $C$ and $D$. Then one can find $A$ and $B$ from Eqs. (A3) and (A4).


[1] M. Maldovan, Nature (London) **503**, 209 (2013).
[2] N. Li, J. Ren, L. Wang, G. Zhang, P. Hänggi, and B. Li, Rev. Mod. Phys. **84**, 1045 (2012).
[3] Y.-F. Ding, G.-M. Zhu, X.-Y. Shen, X. Bai, and B.-W. Li, Chinese Phys. B **31**, 126301 (2022).
[4] Q. Zhu, K. Zdrojewski, L. Castelli, and G. Wehmeyer, Adv. Funct. Mater. **32**, 2206733 (2022).
[5] B. Li, L. Wang, and G. Casati, Appl. Phys. Lett. **88**, 143501 (2006).
[6] K. Joulain, J. Drevillon, Y. Ezzahri, and J. Ordonez-Miranda, Phys. Rev. Lett. **116**, 200601 (2016).
[7] B. Li, L. Wang, and G. Casati, Phys. Rev. Lett. **93**, 184301 (2004).
[8] B. Liu, J. A. Baimova, C. D. Reddy, S. V. Dmitriev, W. K. Law, X. Q. Feng, and K. Zhou, Carbon **79**, 236 (2014).
[9] A. V. Savin, Phys. Rev. B **100**, 245415 (2019).
[10] S. Hu, M. An, N. Yang, and B. Li, Small **13**, 1602726 (2017).
[11] Z. Duan, D. Liu, G. Zhang, Q. Li, C. Liu, and S. Fan, Small **9**, 3133 (2017).
[12] H. Zhao, X. Yang, C. Wang, R. Lu, T. Zhang, H. Chen, and X. Zheng, Mater. Today Phys. **30**, 100941 (2023).
[13] F. Malik and K. Fobelets, J. Semicond. **43**, 103101 (2022).
[14] N. Roberts and D. Walker, Int. J. Therm. Sci. **50**, 648 (2011).
[15] H. Liu, H. Wang, and X. Zhang, Appl. Sci. **9**, 344 (2019).
[16] T. J. Shimokusu, Q. Zhu, N. Rivera, and G. Wehmeyer, Int. J. Heat Mass Transf. **182**, 122035 (2022).
[17] J. Miller, W. Jang, and C. Dames, Proc. ASME Summer Heat Transf. Conf. **2**, 317 (2009).
[18] L. Wang and B. Li, Phys. Rev. Lett. **99**, 177208 (2007).
[19] A. Fornieri, C. Blanc, R. Bosisio, S. D'Ambrosio, and F. Giazotto, Nat. Nanotechnol. **11**, 258 (2016).
[20] S. Murad and I. K. Puri, Appl. Phys. Lett. **102**, 193109 (2013).
[21] M. Peyrard, Europhys. Lett. **76**, 49 (2006).
[22] M. Terraneo, M. Peyrard, and G. Casati, Phys. Rev. Lett. **88**, 094302 (2002).
[23] J. J. Wang, J. Gong, A. J. H. McGaughey, and D. Segal, J. Chem. Phys. **157**, 174105 (2022).
[24] C. Zhang, Z. Guo, and S. Chen, Int. J. Heat Mass Transf. **153**, 119665 (2020).
[25] Z. Yu, L. Ferrer-Argemi, and J. Lee, J. Appl. Phys. **122**, 244305 (2017).
[26] J. Lee, W. Lee, G. Wehmeyer, S. Dhuey, D. Olynick, S. Cabrini, C. Dames, J. Urban, and P. Yang, Nat. Commun. **8**, 14054 (2017).
[27] N. Roberts and D. Walker, J. Heat Transf. **133**, 092401 (2011).
[28] Y. Ammar, S. Joyce, R. Norman, Y. Wang, and A. Roskilly, Appl. Energy **89**, 3 (2012).
[29] A. Luo, H. Fang, J. Xia, B. Lin, and Y. Jiang, Resour. Conserv. Recycl. **125**, 335 (2017).
[30] N. Gangar, S. Macchietto, and C. N. Markides, Energies **13**, 2560 (2020).
[31] S. A. Omer, S. B. Riffat, and X. Ma, Appl. Therm. Eng. **21**, 1265 (2001).
[32] Z. Meng, R. Gulfam, P. Zhang, and F. Ma, Int. J. Therm. Sci. **164**, 106856 (2021).
[33] Z. Meng, R. Gulfam, P. Zhang, and F. Ma, Int. J. Heat Mass Transf. **147**, 118915 (2020).
[34] N. Kalantar, B. K. Agarwalla, and D. Segal, Phys. Rev. E **103**, 052130 (2021).
[35] N. Kalantar, B. K. Agarwalla, and D. Segal, J. Chem. Phys. **153**, 174101 (2020).
[36] T. Hu, K. Hu, and Y. Tang, Int. J. Mod. Phys. B **26**, 1250046 (2012).
[37] A. Maznev, A. Every, and O. Wright, Wave Motion **50**, 776 (2013).
[38] P. E. Hopkins and J. R. Serrano, Phys. Rev. B **80**, 201408(R) (2009).
[39] S. H. S. Silva, Theor. Mat. Phys. **204**, 918 (2020).
[40] S. Lepri, R. Livi, and A. Politi, Phys. Rep. **377**, 1 (2003).
[41] A. Dhar, Adv. Phys. **57**, 457 (2008).

[42] D. Saadatmand, D. Xiong, V. A. Kuzkin, A. M. Krivtsov, A. V. Savin, and S. V. Dmitriev, Phys. Rev. E **97**, 022217 (2018).
[43] D. Xiong, D. Saadatmand, and S. V. Dmitriev, Phys. Rev. E **96**, 042109 (2017).
[44] J. Wang, S. V. Dmitriev, and D. Xiong, Phys. Rev. Res. **2**, 013179 (2020).
[45] S. You, D. Xiong, and J. Wang, Phys. Rev. E **101**, 012125 (2020).
[46] D. Xiong and Y. Zhang, Phys. Rev. E **98**, 012130 (2018).
[47] D. Xiong, Phys. Rev. E **97**, 022116 (2018).
[48] S. Bhattacharyya and P. K. Patra, Commun. Nonlinear Sci. Numer. Simulat. **90**, 105323 (2020).
[49] D. S. Sato, Phys. Rev. E **102**, 012111 (2020).
[50] J. Wang, T.-x. Liu, X.-z. Luo, X.-L. Xu, and N. Li, Phys. Rev. E **101**, 012126 (2020).
[51] P. Dugar and C.-C. Chien, Phys. Rev. E **99**, 022131 (2019).
[52] A. A. Sokolov, A. M. Krivtsov, and W. H. Müller, Phys. Mesomech. **20**, 305 (2017).
[53] V. A. Kuzkin and A. M. Krivtsov, Phys. Solid State **59**, 1051 (2017).
[54] V. A. Kuzkin and A. M. Krivtsov, Dokl. Phys. **62**, 85 (2017).
[55] A. M. Krivtsov, M. B. Babenkov, and D. V. Tsvetkov, Phys. Mesomech. **23**, 109 (2020).
[56] A. M. Krivtsov, Dokl. Phys. **60**, 407 (2015).
[57] V. A. Kuzkin and A. M. Krivtsov, J. Phys.: Condens. Matter **29**, 505401 (2017).
[58] V. A. Kuzkin and A. M. Krivtsov, J. Micromech. Mol. Phys. **03**, 1850004 (2018).
[59] J. Chen, X. Xu, J. Zhou, and B. Li, Rev. Mod. Phys. **94**, 025002 (2022).
[60] J. Chen, J. He, D. Pan, X. Wang, N. Yang, J. Zhu, S. Yang, and G. Zhang, Sci. China Phys. Mech. Astron. **65**, 117002 (2022).
[61] J. Behera and M. Bandyopadhyay, Phys. Rev. E **104**, 014148 (2021).
[62] J. Zhao, D. Wei, Y. Dong, D. Zhang, and D. Liu, Int. J. Heat Mass Transf. **194**, 123024 (2022).
[63] V. Upadhyay, M. T. Naseem, R. Marathe, and O. E. Müstecaplloğlu, Phys. Rev. E **104**, 054137 (2021).
[64] K. H. Lee, V. Balachandran, and D. Poletti, Phys. Rev. E **103**, 052143 (2021).
[65] L. Defaveri and C. Anteneodo, Phys. Rev. E **104**, 014106 (2021).
[66] C.-C. Chien, S. Kouachi, K. A. Velizhanin, Y. Dubi, and M. Zwolak, Phys. Rev. E **95**, 012137 (2017).
[67] A. V. Savin, Y. S. Kivshar, and B. Hu, Phys. Rev. B **82**, 195422 (2010).
[68] A. V. Savin, in *Carbon Nanomaterials: Modeling, Design, and Applications*, edited by K. Zhou (CRC, Boca Raton, 2019).
[69] G. Zhang and Y.-W. Zhang, Chinese Phys. B **26**, 034401 (2017).
[70] Z. Zhangz, Y. Ouyang, J. Chen, and S. Volz, Chinese Phys. B **29**, 124402 (2020).
[71] W. Ren, Y. Ouyang, P. Jiang, C. Yu, J. He, and J. Chen, Nano Lett. **21**, 2634 (2021).
[72] P. Jiang, Y. Ouyang, W. Ren, C. Yu, J. He, and J. Chen, APL Mater. **9**, 040703 (2021).
[73] Z. Wang, M. An, K. Zhang, D. Chen, X. Sun, X. Wang, Y. Yuan, J. Shi, and J. Wu, Surf. Interfaces **36**, 102603 (2023).
[74] R. V. Goldstein and N. F. Morozov, Phys. Mesomech. **10**, 235 (2007).
[75] V. A. Kuzkin, Phys. Rev. E **107**, 065004 (2023).
[76] A. M. Krivtsov, Z. Angew. Math. Mech. **103**, e202100496 (2023).
[77] J. M. Ziman, *Electrons and Phonons: The Theory of Transport Phenomena in Solids* (Oxford University Press, Oxford, 2001).
[78] A. A. Samarskij and E. S. Nikolaev, *Numerical Methods for Grid Equations* (Birkhauser, Basel, 1989), Vol. I.
[79] N. S. Bakhvalov, *Numerical Methods: Analysis, Algebra, Ordinary Differential Equations* (MIR, Moscow, 1977).
[80] X. Ding and Y. Ming, Chinese Phys. Lett. **31**, 046601 (2014).
[81] V. A. Kuzkin and A. M. Krivtsov, Phys. Rev. E **101**, 042209 (2020).
[82] E. A. Korznikova, V. A. Kuzkin, A. M. Krivtsov, D. Xiong, V. A. Gani, A. A. Kudreyko, and S. V. Dmitriev, Phys. Rev. E **102**, 062148 (2020).
[83] S. D. Liazhkov and V. A. Kuzkin, Phys. Rev. E **105**, 054145 (2022).
[84] V. A. Kuzkin and S. D. Liazhkov, Phys. Rev. E **102**, 042219 (2020).
[85] E. A. Podolskaya, A. M. Krivtsov, and V. A. Kuzkin, in *Mechanics and Control of Solids and Structures*, edited by V. A. Polyanskiy and A. K. Belyaev, Advanced Structured Materials Vol. 164 (Springer International, Cham, 2022), pp. 501–533.
[86] O. S. Loboda, A. M. Krivtsov, A. V. Porubov, and D. V. Tsvetkov, Z. Angew. Math. Mech. **99**, e201900008 (2019).
[87] S. N. Gavrilov and A. M. Krivtsov, Continuum Mech. Thermodyn. **34**, 297 (2022).
[88] A. Y. Panchenko, V. A. Kuzkin, and I. E. Berinskii, J. Phys.: Condens. Matter **34**, 165402 (2022).
[89] A. V. Savin and Y. S. Kivshar, Phys. Rev. B **105**, 205414 (2022).